TABLE OF CONTENTS

	Page	
SYMBOLS	v	1/A7
SUMMARY	1	1/A9
INTRODUCTION	1	1/A9
FLIGHTPATH SPECIFICATION AND COMPUTATION	3	1/A11
EVALUATION OF PERFORMANCE ON A GIVEN APPROACH PATH	7	1/B1
The Performance Index	7	1/B1
Calculation of Fuel Flow Rate for a Given Flight Condition	7	1/B1
Approach Path Segments With Approximately Constant Flight Conditions	10	1/B4
Fuel Consumption	12	1/B6
DATA MATRIX FOR THE APPROACH PATH OPTIMIZATION	12	1/B6
RESULTS AND DISCUSSION		
Straight-Line Segment	13	1/B7
180° Turn	15	1/B9
Approach With ψ = 180° and One Deceleration Segment	16	1/B10
Approach With ψ = 180° and Two Deceleration Segments	16	1/B10
Results for All Approaches	19	1/B13
Flight-Test Verification of Analytical Results	25	1/C5
Analytical Results for a CTOL Jet	25	1/C5
SUMMARY AND CONCLUSIONS	28	1/C8
APPENDIX	29	1/C9
REFERENCES	32	1/C12

APR 8 1980
Item 830-4-15
NAS1.60:1650
COMPLETED
ORIGINAL

NASA Technical Paper 1650

Analysis of Fuel-Conservative Curved Decelerating Approach Trajectories for Powered-Lift and CTOL Jet Aircraft

Frank Neuman

APRIL 1980

NASA

40

NASA Technical Paper 1650

Analysis of Fuel-Conservative Curved Decelerating Approach Trajectories for Powered-Lift and CTOL Jet Aircraft

Frank Neuman
Ames Research Center
Moffett Field, California

National Aeronautics
and Space Administration

**Scientific and Technical
Information Office**

1980

TABLE OF CONTENTS

	Page
SYMBOLS	v
SUMMARY	1
INTRODUCTION	1
FLIGHTPATH SPECIFICATION AND COMPUTATION	3
EVALUATION OF PERFORMANCE ON A GIVEN APPROACH PATH	7
The Performance Index	7
Calculation of Fuel Flow Rate for a Given Flight Condition	7
Approach Path Segments With Approximately Constant Flight Conditions	10
Fuel Consumption	12
DATA MATRIX FOR THE APPROACH PATH OPTIMIZATION	12
RESULTS AND DISCUSSION	
Straight-Line Segment	13
180° Turn	15
Approach With ψ = 180° and One Deceleration Segment	16
Approach With ψ = 180° and Two Deceleration Segments	16
Results for All Approaches	19
Flight-Test Verification of Analytical Results	25
Analytical Results for a CTOL Jet	25
SUMMARY AND CONCLUSIONS	28
APPENDIX	29
REFERENCES	32

SYMBOLS

A - I	points on the approach trajectory
A	starting point
a	acceleration, m/sec
B, C	begin and end of turn to final
D, E, F, C	begin and end of first and second deceleration
H, I	begin and end of descent
D	drag, N
$\dot{E}_n$	nondimensionalized energy rate
f	total fuel consumed, kg
f( )	functional relationship
$\dot{f}$	fuel flow rate, kg/sec
g	acceleration of gravity, m/sec
h_N	altitude at Point N on the trajectory, m
k	constant in the performance index, kg
L	lift (aerodynamic plus propulsive), N
PI	performance index
R	radius of turn, m
S	distance along the trajectory, m
S_{MN}	distance between Points N and M on the trajectory, m
T	thrust component relative to the longitudinal axis, N
t	time of flight, sec
V_N	true airspeed at Point N on the trajectory, m/sec
$\dot{V}_a$	acceleration with respect to the air mass, m/sec
W	weight, kg

W_x, W_y	wind in the x and y direction, m/sec
W_T	tailwind component, m/sec
X	minimum distance from line 00' to C
Δ	change in a quantity
γ_a	aerodynamic flightpath angle, deg
γ_I	inertial flightpath angle, deg
ϕ	bank angle, deg
ψ	heading change in the turn, deg

ANALYSIS OF FUEL-CONSERVATIVE CURVED DECELERATING APPROACH TRAJECTORIES FOR POWERED-LIFT AND CTOL JET AIRCRAFT

Frank Neuman

Ames Research Center

SUMMARY

This paper describes a method for determining fuel-conservative terminal approaches that include changes in altitude, speed, and heading. The horizontal approach trajectory is constrained to a straight segment followed by a constant radius turn; the vertical trajectory is constrained to level flight plus one descending segment with constant inertial flightpath angle; and the speed profile is constrained to a maximum of two deceleration segments. Simulation results for the Augmentor Wing Jet STOL Research Aircraft and for the Boeing 727 aircraft indicate that for minimum fuel consumption, two deceleration segments are required: one terminates at the end of the straight-line approach and the other at the end of the turn. Deceleration should be at the highest practical rate for minimum fuel consumption. The choice of a specific glide-slope angle has a small effect on the total amount of fuel consumed as long as the altitude change is small. For most conditions, the descent should be completed before the first deceleration is started. However, choosing the descent to terminate at the end of the turn in order to minimize community noise levels results in a penalty of only a few kilograms of fuel. For comparison, a trajectory optimized for a single deceleration segment requires about 21 kg more fuel than the optimal two-deceleration approach. These results were verified by flight tests using the Augmentor Wing Aircraft. Additional fuel savings possible through variable radius turns are discussed in the appendix.

INTRODUCTION

Powered-lift STOL aircraft have the potential to reduce congestion at hub airports and to operate quietly near populated areas. These advantages are achieved at the cost of higher fuel consumption during terminal area approaches while operating in the powered-lift STOL configuration. Since these aircraft will spend a relatively large percentage of their flight time in the terminal area (because of their short stage length), it is essential that their fuel consumption and flight time in the terminal area be minimized. Research by NASA is in progress to develop techniques for the design of guidance systems that will optimize the effectiveness of STOL aircraft in terminal area operations.

Three different guidance system concepts for STOL aircraft were evaluated in flight: (1) a fixed-trajectory system (ref. 1), (2) a system that included a fixed path and a real-time synthesized capture flightpath (refs. 2, 3), and (3) a trajectory synthesizing system (ref. 4). The fixed-trajectory system uses different classes of way points to specify the three-dimensional path (consisting of straight lines and circular arcs) and the beginning and end of speed changes. Although this allows great flexibility in specifying trajectories, it does not provide information on the best way of selecting trajectories or on how to capture them at a specified point in space and time. These procedures were left to the judgment of pilots and operators. The second system solved the capture problem by synthesizing in real time a turn-straight-turn minimum-time flightpath from an aircraft position to any way point on the fixed flightpath. In the third system, real-time synthesis of the vertical and speed profiles were added to the solution of the capture problem. This synthesis, which made use of a compact performance model of the aircraft, was based on the general characteristics of fuel-efficient, low-noise trajectories; such trajectories require that the start of deceleration and descent be delayed as long as possible. This procedure resulted in near optimality for straight approaches. Erzberger and McLean (ref. 4) used this result in Augmentor Wing flight tests with curved paths, but its optimality for curved paths was not known. This report describes a technique for optimizing curved decelerating and descending terminal-area paths.

Several methods are available for flightpath optimization. The most general method is optimal control and the calculus of variations (ref. 5). This method makes no assumptions about the structure of the trajectories but is difficult to apply for the five-state, four-control, nonlinear system under study. A less general method is to parameterize the structure of the trajectories and then to optimize the trajectories with respect to the parameters. That method was found to be appropriate here because (1) of reduced computation complexity and the simplicity of including operational constraints and (2) parametric description of the flightpath is the method used in RNAV systems today. In addition, the problem was simplified by using the energy rate concept developed by Erzberger and McLean (ref. 4), which reduced the number of controls from four to one.

The essential assumptions for the parametrization of the approach flightpath are the following: use only two flightpath segments in the horizontal plane, a straight line followed by a turn to the final approach; allow a maximum of one deceleration segment in each of these flightpath segments; and permit only one constant flightpath angle segment in the vertical plane for altitude change. (This latter segment might extend over part of the straight segment, the turn, or both.)

Results of this study can be used in the design of flightpaths for fixed-trajectory systems, such as in reference 1, or they can be incorporated in the trajectory synthesis logic of a system, such as that studied in reference 4. As shown in the final section, the results of this study can also be used to effect similar fuel savings for CTOL aircraft.

FLIGHTPATH SPECIFICATION AND COMPUTATION

The problem of determining a fuel-efficient, curved decelerating approach was formulated to limit the design to inertially referenced straight and constant-radius path segments. This formulation of the problem was chosen so the results could be directly verified on an existing RNAV system (such as the STOLAND RNAV system of ref. 4). A subset of all possible approach flightpaths, defining a performance index (e.g., minimum fuel) was selected, and a procedure developed that finds the best flightpath of the subset. The latter involves iteration of the following three steps:

1. The flightpath is specified by means of a few parameters.

2. The fuel used for the flightpath specified in (1) is calculated with the energy rate method (to be described later).

3. A procedure is chosen to alter the flightpath parameters in a systematic way to find the best flightpath (the one with the minimum performance index).

The flightpaths studied here are restricted further to two legs: (1) a long straight segment A-B followed by (2) a constant-radius turn of ψ from the aircraft heading to the runway heading, where $0 < \psi \leq 180°$ (see fig. 1 for a 60° and 120° turn), and where X is fixed at 21,340 m. This distance is representative of a terminal area approach and is sufficiently long that in all cases studied the optimization results are independent of X.

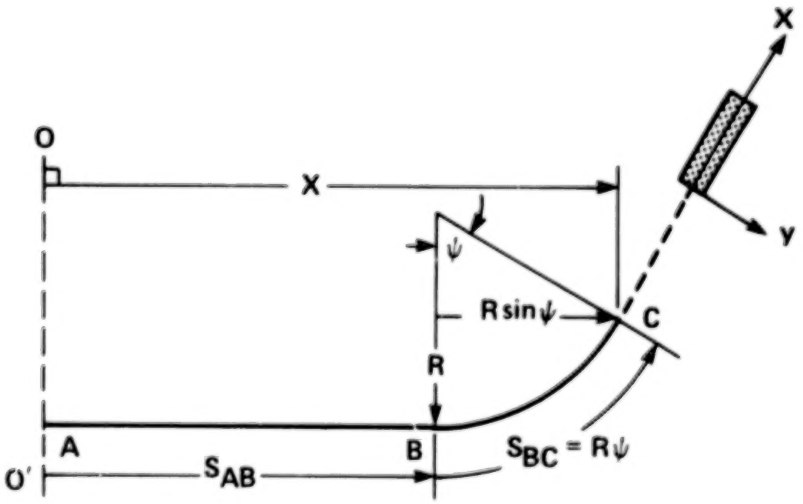

(a) $\psi = 60°$

Figure 1.- Horizontal approach profile.

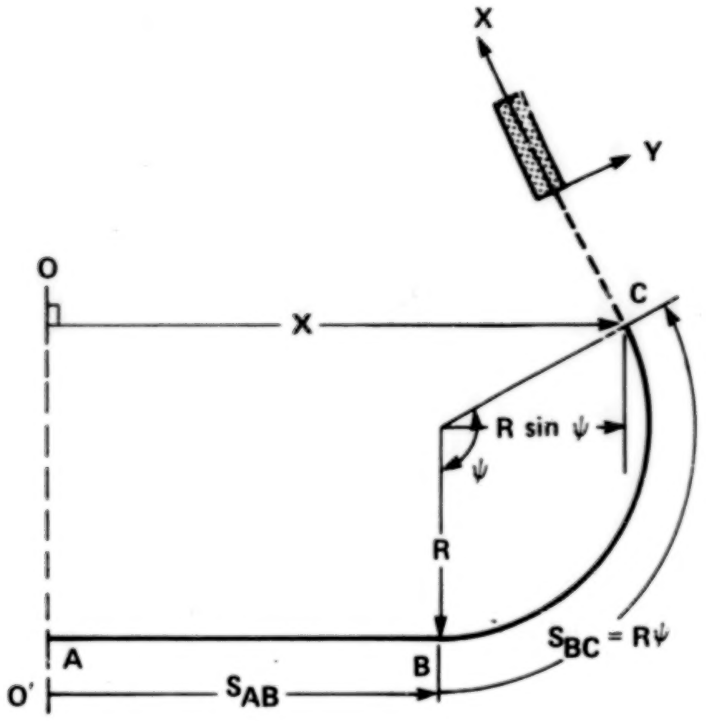

(b) $\psi = 120°$

Figure 1.- Concluded.

Aircraft arriving at Point A are assumed to come from a long distance from the direction of A-B. Hence, there is no fuel penalty in arriving at the prescribed A from the aircraft's origin. Note that A shifts along O - O' as a result of changing R in the optimization process.

For most examples, the boundary conditions are the same. At Point A, the aircraft has an altitude of 610 m and an airspeed of 140 knots. At Point C, the aircraft is at the runway heading, at an altitude of 293 m, has a landing airspeed of 73 knots, and is on a 7° glide slope. For $\psi < 180°$, a part of X is covered by S_{BC}. This is taken into consideration in the computations of fuel optimization by subtracting the length R sin ψ from X for the straight-line section S_{AB}.

$$S_{AB} = X - R \sin \psi \qquad 0 < \psi \leq 180° \tag{1}$$

A speed profile must be defined in terms of way points to meet the end conditions. Two types of speed profiles will be considered. The simplest profile considered here consists of a single deceleration segment (fig. 2) with a constant rate of deceleration. When the starting point D (which is freely selected in the optimization), the deceleration a, and the wind components W_x and W_y are given, the deceleration distance S_{DE} and the airspeed V_B at which the turn is entered can be calculated. When D and E are both on the straight-line portion of the flightpath S_{AB},

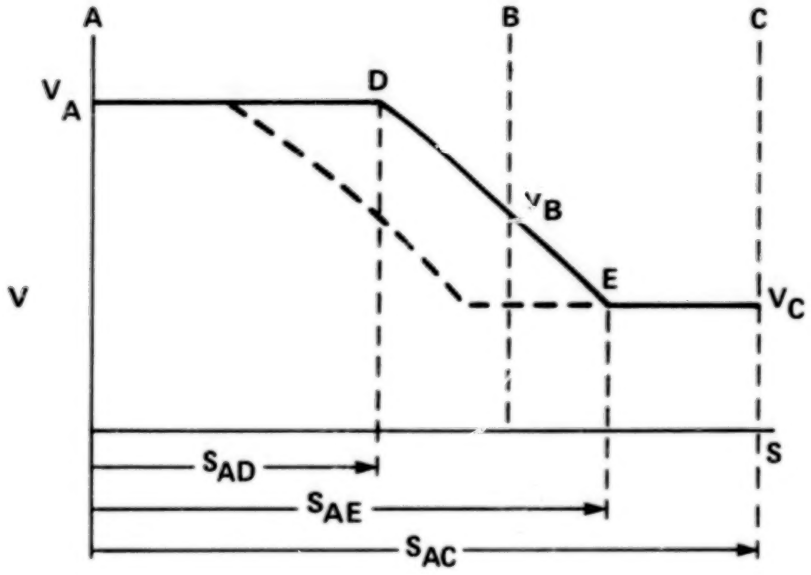

Figure 2.- Single-deceleration profile.

$$S_{DE} = \left(\frac{V_C + V_A}{2} + W_T\right) \frac{V_C - V_A}{a} \tag{2}$$

where W_T is the wind component along the flightpath.

If $S_{AE} = S_{AD} + S_{DE} < S_{AB}$ then $V_B = V_C$. However, if $S_{AD} < S_{AB}$ and $S_{AE} > S_{AB}$, as in figure 2, then one must calculate V_B,

$$V_B = -W_T + \sqrt{(V_A + W_T)^2 + 2aS_{DB}} \tag{3}$$

and S_{BE} must be calculated by numerical integration by breaking the velocity difference V_B to V_C into small segments and considering the variation in tailwind with the change in heading. The radius of the turn is determined by

$$R = \frac{(V_B + W)^2}{g \tan \phi_n} \tag{4}$$

where $W = 20$ knots has been added to V_B to account for unknown winds, ϕ_n = nominal bank angle of 20°, and $g = 9.81$ m/sec. (Since the maximum bank angle allowable in the STOLAND system is 30°, the actual wind that the system can handle is substantially higher than 20 knots.)

The R chosen above is the minimum (wind-proofed) constant-radius turn for the given entry speed V_B. Other choices are possible, such as using the measured wind in equation (4) instead of W, or the maximum tailwind component based on the measured wind. These have not been chosen for this study, since STOLAND on-board wind estimates are not very accurate. Choosing the minimum radius of turn *for the given speed* V_B to accomplish the required

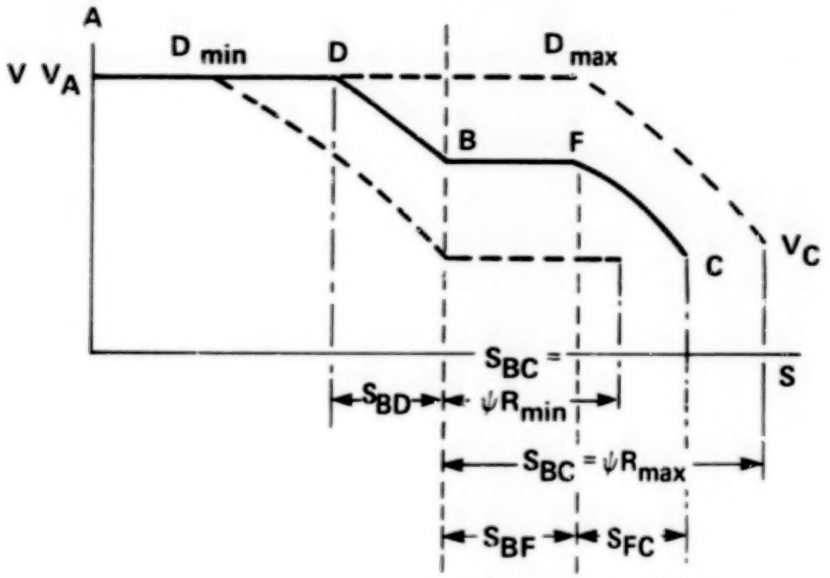

Figure 3.- Two-deceleration speed profile.

heading change ensures minimum fuel in the turn because the increase in path length for larger radii turns always increases the total amount of fuel used in the turn, even though there is a second-order reduction in fuel consumed per meter due to the shallower bank angle.

A more complex speed profile contains two deceleration segments (fig. 3). For this investigation, the first decelerating segment was restricted to end at Point B and the second at Point C. (That this is a reasonable restriction will become clear in the discussion of results.) The limits of variation of D are sketched in figure 3, which also shows the effect of V_B on S_{BC}. Again equations (2) to (4) apply and S_{FC} is calculated by numerical integration.

Once the speed profile is determined, one must also determine the altitude profile. The aircraft must descend from an initial altitude at A (h_A) to a final altitude at I (h_C) (fig. 4). With a given inertial flightpath angle γ_I, h_A, and h_C determine S_{HI} from the relation

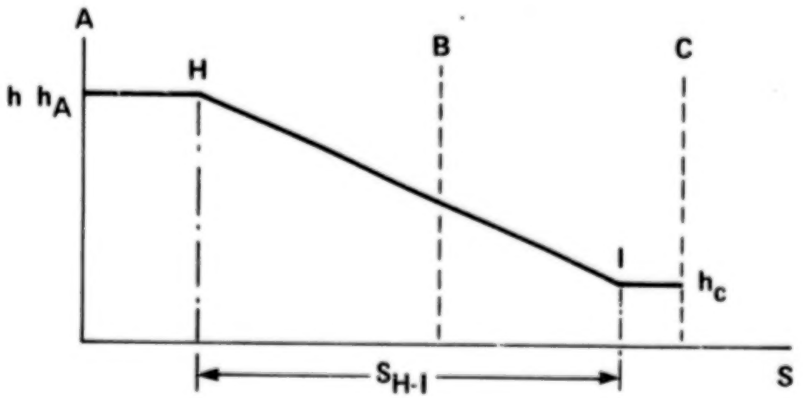

Figure 4.- Altitude profile.

$$S_{HI} = \frac{-(h_A - h_C)}{\tan \gamma_I} \tag{5}$$

From the above discussion, the following parameters define the flightpath. The fixed parameters in the problem are X, V_A, V_C, h_A, h_C, and ψ; the variable parameters are S_{AD}, S_{AH}, a, and γ_I, which are chosen to optimize the performance functions; and the derived parameters are V_B, S_{DE}, S_{HI}, and R (eqs. (2) to (5)). The variable parameters S_{AD}, S_{AH}, a, and γ_I can be varied within limits to search for an optimum approach flightpath. For the approach study, the variables a and γ_I are limited due to aircraft performance limits $0 \geqslant a \geqslant -0.042$ g, since flap deployment in the Augmentor Wing is slow, and $0 \geqslant \gamma_I > -7.5°$. (It should be noted that in powered flight, nozzles could be used for a higher rate of deceleration; however, that is noisy and fuel-inefficient.) Parameters S_{AD} and S_{AH} are limited so that the decelerations and altitude changes are contained within the length of the flightpath.

EVALUATION OF PERFORMANCE ON A GIVEN APPROACH PATH

The Performance Index

The primary quality criterion chosen was consumed fuel f, but this resulted in large flat areas in the performance index. For example, when deceleration occurred late in the approach, descent could begin and end anywhere in the straight-line segment of the flightpath without affecting f. Hence, a second quality criterion was added to the performance index to favor placing I, the final point of descent, as close as possible to the end point of the flightpath and to favor steep flightpath angles without a large cost of fuel:

$$PI = f + K\left[\frac{\gamma_I}{7.5} - \frac{S_{IC}}{S_{AC}}\right] \quad [kg] \tag{6}$$

where S_{AC} is the total length of the flightpath, f is the fuel used for flying the path, and $K = 1$ kg. This strategy reduces aircraft noise effects on the community surrounding the STOL airport.

Calculation of Fuel Flow Rate for a Given Flight Condition

The calculation of the total fuel consumed on the flightpath is divided into three steps: (1) the fuel flow rates for all possible flight conditions are determined; (2) the approach path is divided into small segments for which the flight conditions are approximately constant; and (3) the fuel for each of the individual segments is calculated and summed over all segments to arrive at the total fuel consumed for the specified approach path. These steps are sketched out in the following sections.

To solve flightpath optimization problems, fuel flow rates for all flight conditions must be known. Erzberger and McLean (ref. 4) have shown that use of a normalized, nondimensional energy rate $\dot{E}_n$ as state variable reduces the computation effort and data storage and that it is a sufficiently good approximation for flightpath optimization work. The energy rate $\dot{E}_n$ for small flightpath angles is:

$$\dot{E}_n \triangleq \frac{a}{g} + \gamma_a = \left.\frac{T - D}{W}\right|_{L=W} \tag{7}$$

Equation (7) shows that the linear combination of acceleration and aerodynamic flightpath angle is related to the required thrust (and hence fuel flow rate) for a given weight, speed, altitude, air density, and temperature (since T and D are functions of the latter four variables). As described in reference 4, for a given $\dot{E}_n$ and V the fuel flow rate and aircraft control positions (throttle angle, nozzle angle, flap angle, and angle of attack) are uniquely determined from the mathematical aircraft model of the Augmentor Wing such that the fuel flow rate is minimum. Operational restrictions such as maneuver margin, deceleration limits, and minimization of ground-perceived aircraft noise are included in this minimization process.

An example of fuel flow rate vs speed, with $\dot{E}_n$ as a parameter, is shown in figure 5 for the Augmentor Wing Jet STOL Research Aircraft. Control positions are not shown, nor are they needed, since they are replaced in this analysis by the energy rate variable. (Control positions as a function of energy rate are needed for on-board implementation.) Figure 5 shows that, at a given speed, the fuel flow rate decreases with steeper descents and greater decelerations. This expresses the equivalence of potential or kinetic energy with fuel energy for propulsion. Also, when the data are converted from fuel per unit time to fuel per unit distance, the results show that for the range of speeds presented in figure 5, the higher the speed the less fuel is consumed per meter. For the investigation at hand, in which the altitude span is not large, the data in figure 5 will suffice. (The data in fig. 5 are for sea level altitude and standard day temperature and pressure.) More generally, by the methods described in reference 5, data for all aircraft weights, terminal area altitudes, and atmospheric conditions can be derived.

The data in figure 5 must be corrected for the effect of the additional lift required in a turn. For a coordinated turn, the lift force-balance equation is

$$L = \frac{W \cos \gamma_a}{\cos \phi_a} \tag{8}$$

Hence, the effect of a turn on the solution for the required control settings is approximately equivalent to increasing the weight of the aircraft in a straight approach by

$$\Delta W = W \left(\frac{1}{\cos \phi} - 1\right) \tag{9}$$

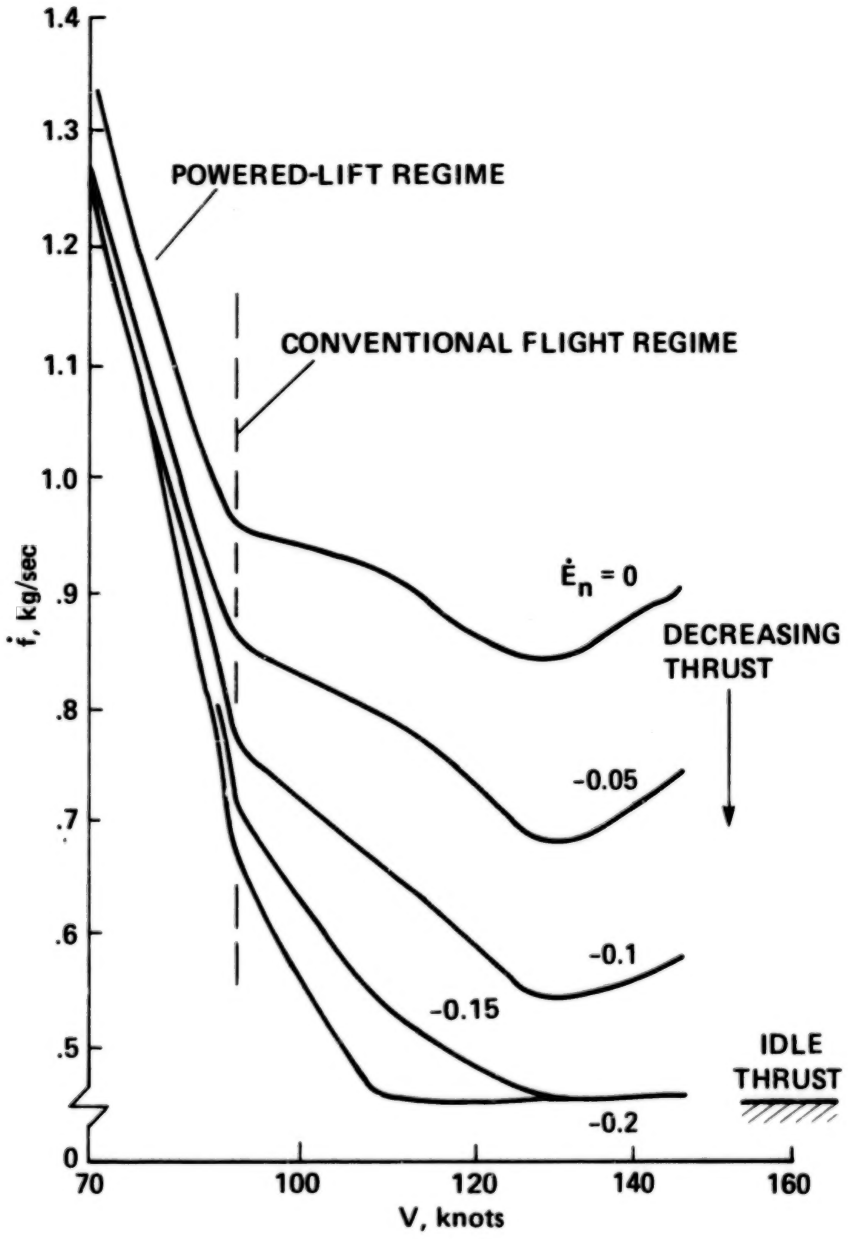

Figure 5.- Fuel flow rate vs airspeed for the Augmentor Wing Aircraft at sea level, standard day temperature and pressure, at an aircraft weight of 20,412 kg.

Fuel flow rates at the nominal roll angle of 20° were determined. The differences between them and the results in figure 5 are shown in figure 6. The additional fuel flow rate increases with a decrease in speed, because more of the required vertical force must be supplied by engine thrust. The additional fuel flow rate for any bank angle is approximated as

$$\Delta\dot{f} = \frac{\Delta W(\phi)}{\Delta W(20°)} \quad \Delta\dot{f}(20°) \tag{10}$$

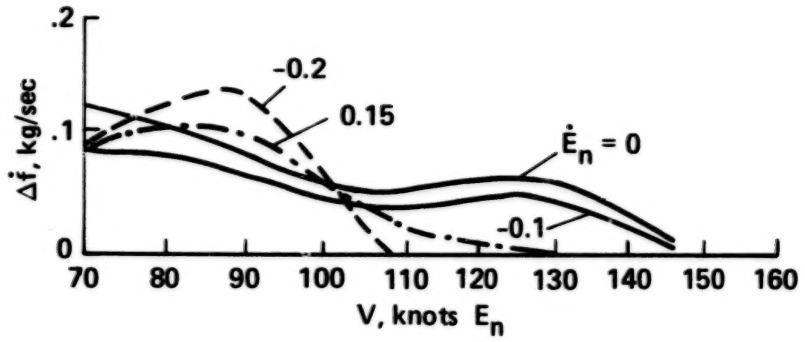

Figure 6.- Incremental fuel flow rate for $\phi = 20°$.

Approach Path Segments With Approximately Constant Flight Conditions

The fuel flow rate must be integrated to obtain the fuel used for the complete flightpath. First, a single deceleration path or a two deceleration path is specified from a minimum amount of input data, such as S_{AD} and S_{AH}, as explained in the last section. Then the points D, E, H, and I are ordered along S. Because segments DE and HI are of variable length and location on the trajectory, six different orders of the points can occur on the straight segment, each requiring a different sequence of computations:

A D E H I B
A D H E I B
A D H I E B
A H D E I B
A H D I E B
A H I D E B

When a point actually occurs beyond B (on the curved segment), its actual distance along the path is replaced by S_{AB}. Thus, for the five segments implied by each of the six orderings, four may be of zero length.

The sequence AHDEIB, shown in figure 7, is used as an example. All changes in glide-slope angle or acceleration occur before the turn. Figure 7(e) shows the energy change during each of the five segments. For four segments, V and $\dot{E}_n$ are constants; in the fifth segment, DE, V varies due to deceleration and $\dot{E}_n$ varies because the wind causes the aerodynamic flightpath angle (eq. (15)) to change during deceleration. In the latter case, the fuel consumed must be calculated by breaking the flightpath into smaller segments for numerical integration.

Numerical integration is also required for the turn — the change in tailwind as the turn progresses makes this necessary for all segments of the turn (even constant airspeed segments). Numerical integration is accomplished by dividing each segment into smaller segments over which the parameters can be assumed to be approximately constant. Given the angle ψ, defined in figure 8 to the center of a small turn segment ($\Delta\psi \leq 15°$), the tailwind is

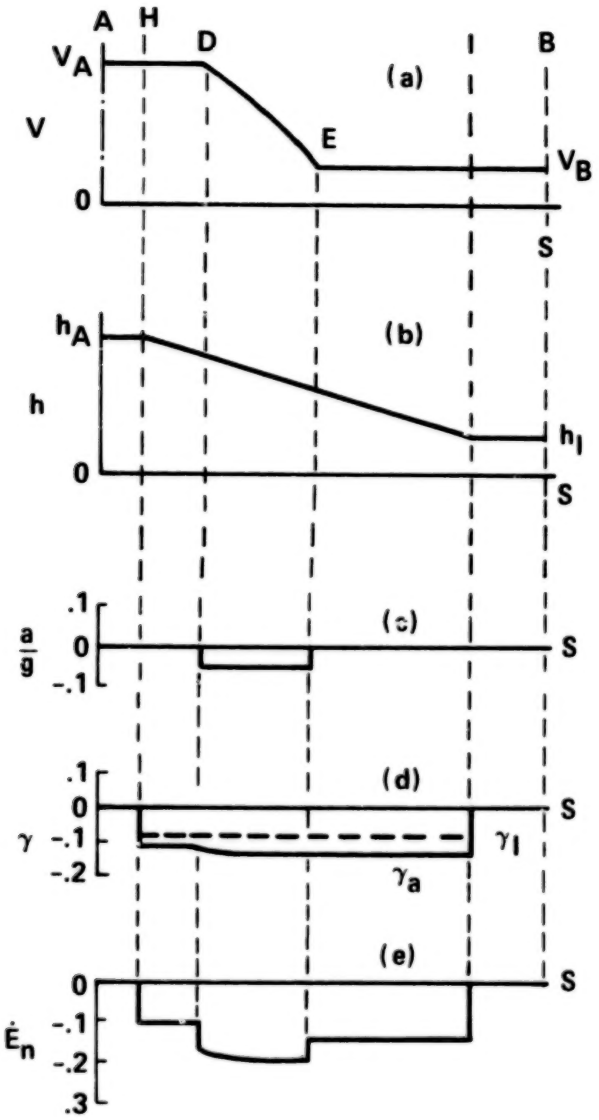

Figure 7.- From speed and altitude profile definitions to $\dot{E}_n$.

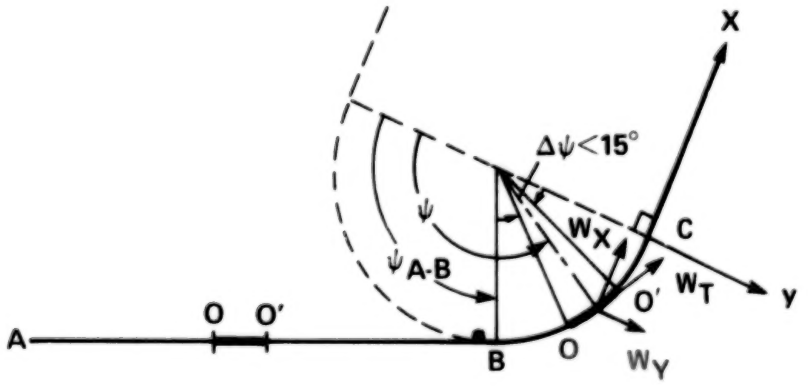

Figure 8.- Geometrical considerations for small turn segment and straight-line segment.

$$W_T = -W_x \cos \psi + W_y \sin \psi \tag{11}$$

(Equation (11) is true for the straight-line segment also, when $\psi = \psi_{AB}$.) Given the speed V at the center of the segment, the roll angle is

$$\phi = \tan^{-1} \frac{(V + W_T)^2}{gR} \tag{12}$$

With the additional information of the deceleration a and inertial flight-path angle γ_I, all information required for calculation of the fuel used in a small segment of the turn is known.

Fuel Consumption

After the path has been divided into segments in which the parameters do not change much, the fuel consumed can be calculated. The average velocity in the segment is

$$\bar{V} = \frac{V_o - V_{o'}}{2} \tag{13}$$

The time on the segment is

$$t = \frac{S_{oo'}}{\bar{V}} \tag{14}$$

and the average aerodynamic glide-slope angle is

$$\gamma_a = \gamma_I \frac{\bar{V} + W_T}{\bar{V}} \tag{15}$$

This information, together with a and the roll angle from equation (12), permits calculations of the fuel consumed in the small segment:

$$f = t\dot{f}(\bar{V}, \dot{E}_n) \tag{16}$$

Equation (16) also holds for large segments, where V and $\dot{E}_n$ do not change. Summation of the fuel consumed in all segments of the approach path gives the total fuel used.

DATA MATRIX FOR THE APPROACH PATH OPTIMIZATION

The above described method was used to evaluate a number of approaches for the Augmentor Wing Aircraft. Six approach paths were chosen with turns of 30°, 60°, 90°, 120°, 150°, and 180°, to cover the range of possible turns. Six wind speeds with respect to the runway heading were chosen: zero wind; headwinds of 40 and 25 knots; side winds of ±15 knots; and a tailwind of

10 knots. These cover the 3σ range of winds specified by the FAA for landing studies. An airspeed reduction from 140 knots to a landing airspeed of 73 knots was chosen. This is typical for the Augmentor Wing Aircraft. The nominal deceleration was 0.042 g, to be slightly below the aircraft deceleration capability in order to permit correction for unknown winds. A $\gamma_I = -7.0°$ glide slope was chosen, since a steep descent tends to minimize noise exposure to the surrounding community. From a preliminary data analysis it was found that the results are not very sensitive to the initial point of descent H. Hence, for the initial search, the final point of descent was selected to be at the end of the turn. This strategy also reduces community noise.

For each of the flightpath-wind combinations, D (fig. 3) was swept through the total range $D_{min} < D \leq D_{max}$ in steps of 300 m. At the smallest fuel value found in the sweep, a search (using consecutively smaller steps) determined D for which fuel was minimum. At this point, the point of descent H was again swept through its total range, followed by a search to find the minimum of the performance index. Occasionally, Jacob's multidimensional search subroutine (ref. 6) was used to find the optimum with several free variables such as a, γ_I, and S_{AD}, while using the values of these variables found in the above procedure as initial values. However, no new answers were obtained by the multidimensional search. To study the sensitivity of the results to other parameters, the above 36 approaches were repeated with two different γ_I's and two different a's.

RESULTS AND DISCUSSION

The approach path is a straight-line segment followed by a turn segment, where each may include a deceleration segment. To provide insight into the optimization of the concatenated flightpath, some data for the variation of fuel with changes with flightpath parameters $f = f(V, a, \gamma_I)$ for the individual path segments will be given and two examples for the complete approach.

Straight-Line Segment

The straight-line segment S_{AB} of figure 1 together with the speed profile shown in figure 9 was chosen since reference 4 showed that when a speed reduction is required in the segment, for minimum fuel, deceleration should occur as late as possible. With the initial speed $V_A = 140$ knots, this is the optimum speed profile, because V_A is the speed of lowest fuel consumption per meter for the Augmentor Wing Aircraft. (Initial speeds that are not fuel-optimum would call for more complex speed profiles.) For the data in figure 9, γ_I and a were varied. Figure 9 shows that the steeper the glideslope angle, the less fuel is used. Also, the larger the deceleration, the less fuel is used; however, the incremental improvement diminishes as the deceleration increases. This is fortunate, since the deceleration limit is 0.042 g.

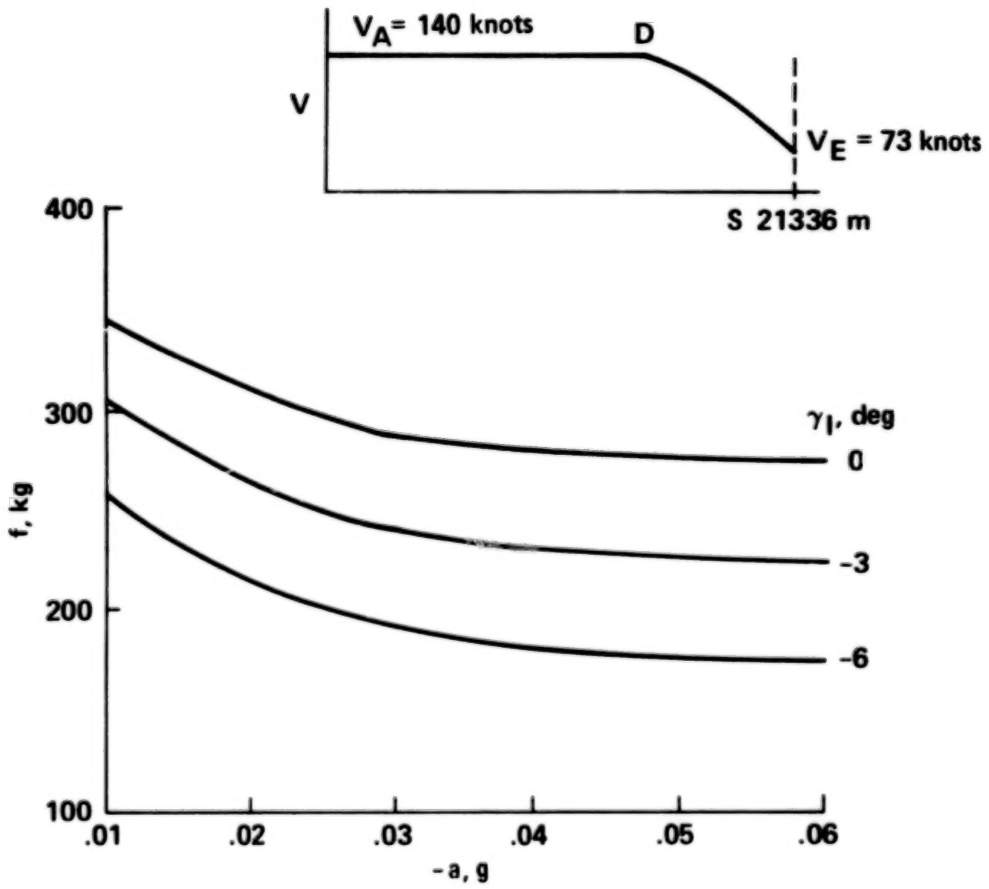

Figure 9.- Fuel for straight flightpath with a deceleration segment (no wind).

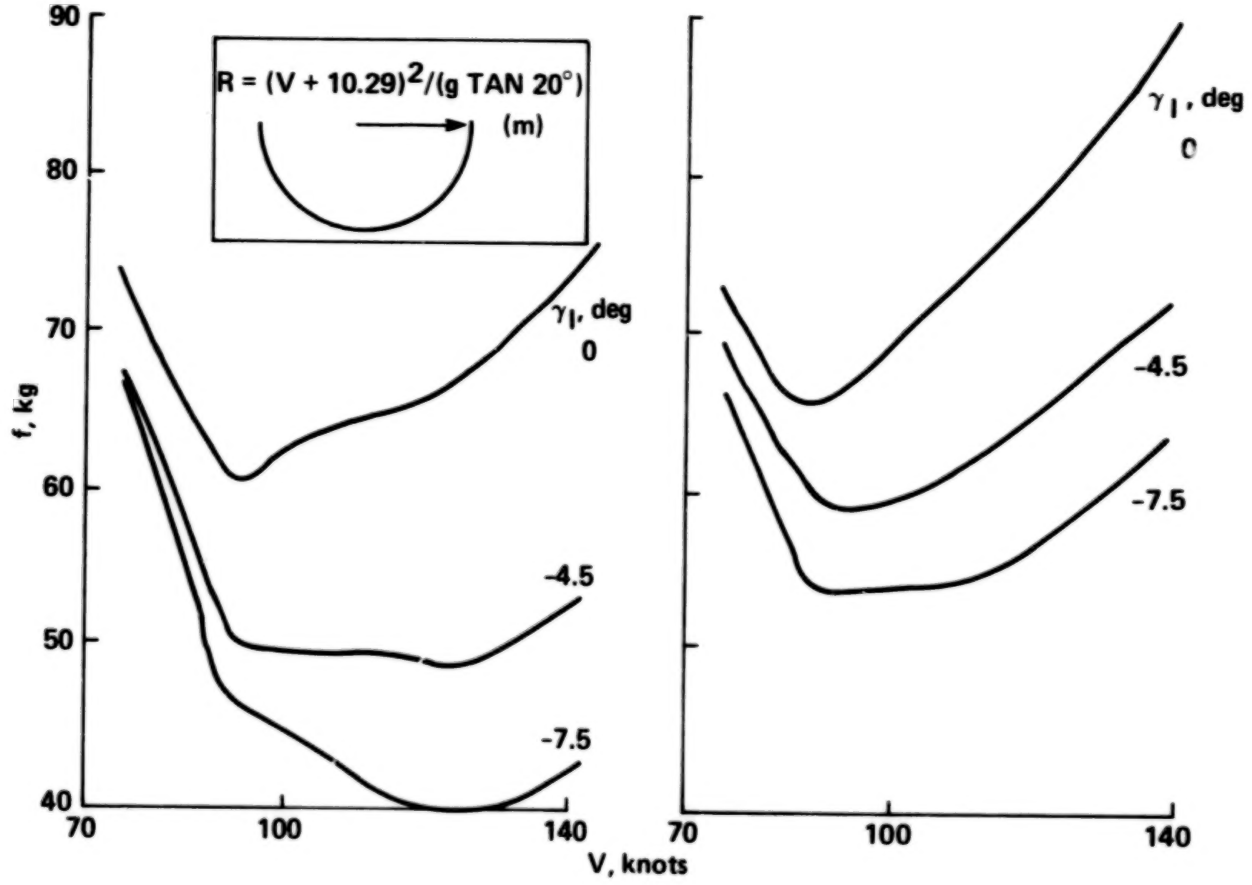

(a) Constant speed turn.

(b) Decelerate to 75 knots at end of turn at a = -0.05 g, V = speed at turn entry.

Figure 10.- Fuel consumption in a 180° turn vs speed V (no wind).

180° Turn

Results for constant speed and decelerating 180° turns are shown in figures 10(a) and 10(b). For both types of turns there is a trade-off between decreased fuel per meter with higher speeds, and shorter path lengths (due to smaller turn radii (eq. (4)) with lower speeds. This results in a minimum of fuel consumption somewhere between the maximum and minimum turn entry speeds. For the constant speed turns, the minimum shifts toward higher speeds as the flightpath angle decreases. For the decelerating turns, the results are plotted for the maximum allowable deceleration (0.05 g for a level turn); the final speed is reached at the end of the turn because, analogous to the straight-line segments, calculations show that this results in the least amount of fuel used. For these decelerating turns (fig. 10(b)) fuel used is increased compared to the constant speed turn, especially for the higher initial speeds. Hence, in figure 10(b) the turn entry speed for minimum fuel does not increase with steeper glide-slope angles, but remains at about 88 knots independent of γ_I.

Approach With $\psi = 180°$ and One Deceleration Segment

For studying the simplest case — a single deceleration segment in the approach flightpath — $\gamma_I = 7.0°$, $a = 0.042$ g, and $I = D$ were chosen (see insert in fig. 11). To change the position of the deceleration segment S_{BE} was varied over the range of interest. For the zero wind case, results (with B chosen as origin) are shown in figure 11. When $S_{AE} < S_{AB}$ (deceleration is contained in the straight segment), the fuel for the turn S_{BC} is independent of S_{BE}; the fuel for the straight segment S_{AB} decreases with increasing S_{BE}. When $S_{AE} > S_{AB}$ but $S_{AD} < S_{AB}$ (deceleration occurs partly in each segment), the turn radius must go up and so does the fuel for the turn (curve 2, fig. 11); the fuel in the straight-line segment decreases further (curve 1, fig. 11), because there is less speed reduction in this segment. Finally, when $S_{AD} > S_{AB}$ (the deceleration segment is contained in the turn), the fuel for the turn begins to decrease, because the maximum turn radius has been reached ($V_B = V_A$). The fuel consumption for the straight segment S_{AB} has some slight increase, because some of the potential energy from descent is now used in the turn. The problem ends when $S_{AE} = S_{AC}$. Curve 3 in figure 11 shows two minima: it takes about the same amount of fuel to decelerate just before the turn and fly a minimum-radius turn (first minimum), as it does to decelerate at the end of the turn and fly a maximum-radius turn (second minimum).

Approach With $\psi = 180°$ and Two Deceleration Segments

In search of further improvements in fuel economy, next we consider a flightpath with two deceleration segments. The two deceleration segments terminate at Points B and C of their respective straight or turn segments. As discussed earlier, this minimizes the fuel for each segment, once the initial and final speeds for the segment are given. By varying the start of the first deceleration D, the problem now remains to find the optimum split of the total speed reduction from approach to landing speed. Figure 3 shows the range of speed profiles considered and the split in deceleration between the two segments, from all in the straight segment to all in the curved segment. For comparison with figure 11, the fuel-consumed curves are shown as functions of S_{FC}, the length of the deceleration segment in the turn. The minimum of the total fuel curve in figure 12 is about 324 kg, which is 21 kg less than the minimum of the corresponding curve in figure 11. The distance S_{FC} corresponding to the minimum of curve 2 is very close to that for the minimum of curve 3. Unfortunately, this is not true for all ψ. Hence, it will not be correct, in general, to minimize the fuel in the decelerating turn and then to precede it with an optimum decelerating straight-line segment that matches the initial speed for this turn. This is expressed in figure 13, where it is shown that V_B, the starting speed at the turn for minimum fuel in the total path, does not agree with the speed that results in minimum fuel in the turn.

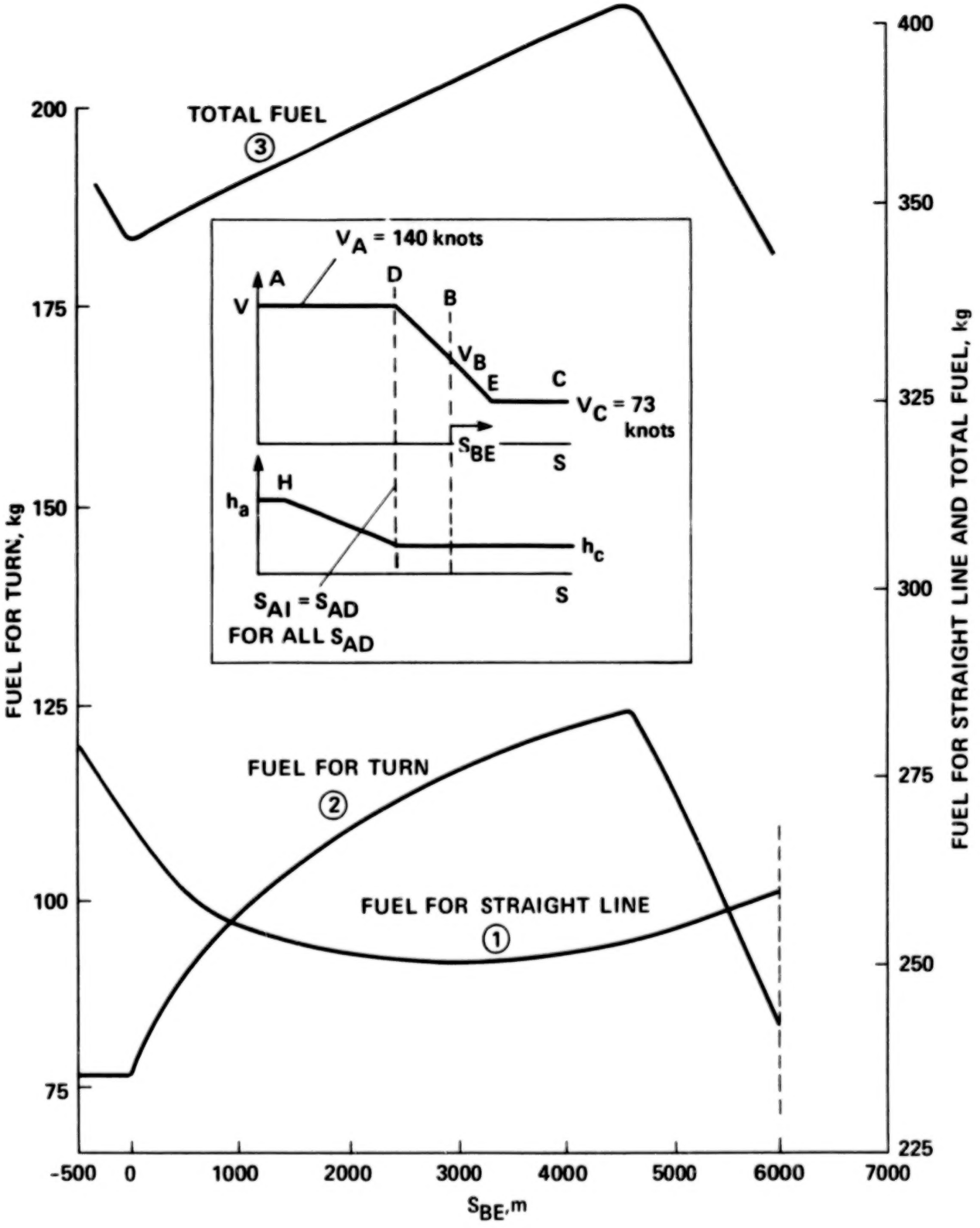

Figure 11.- Fuel for a single-deceleration approach vs S_{BE} (no wind), $\gamma_I = -7°$, a = -0.042 g, $S_{AI} = S_{AD}$.

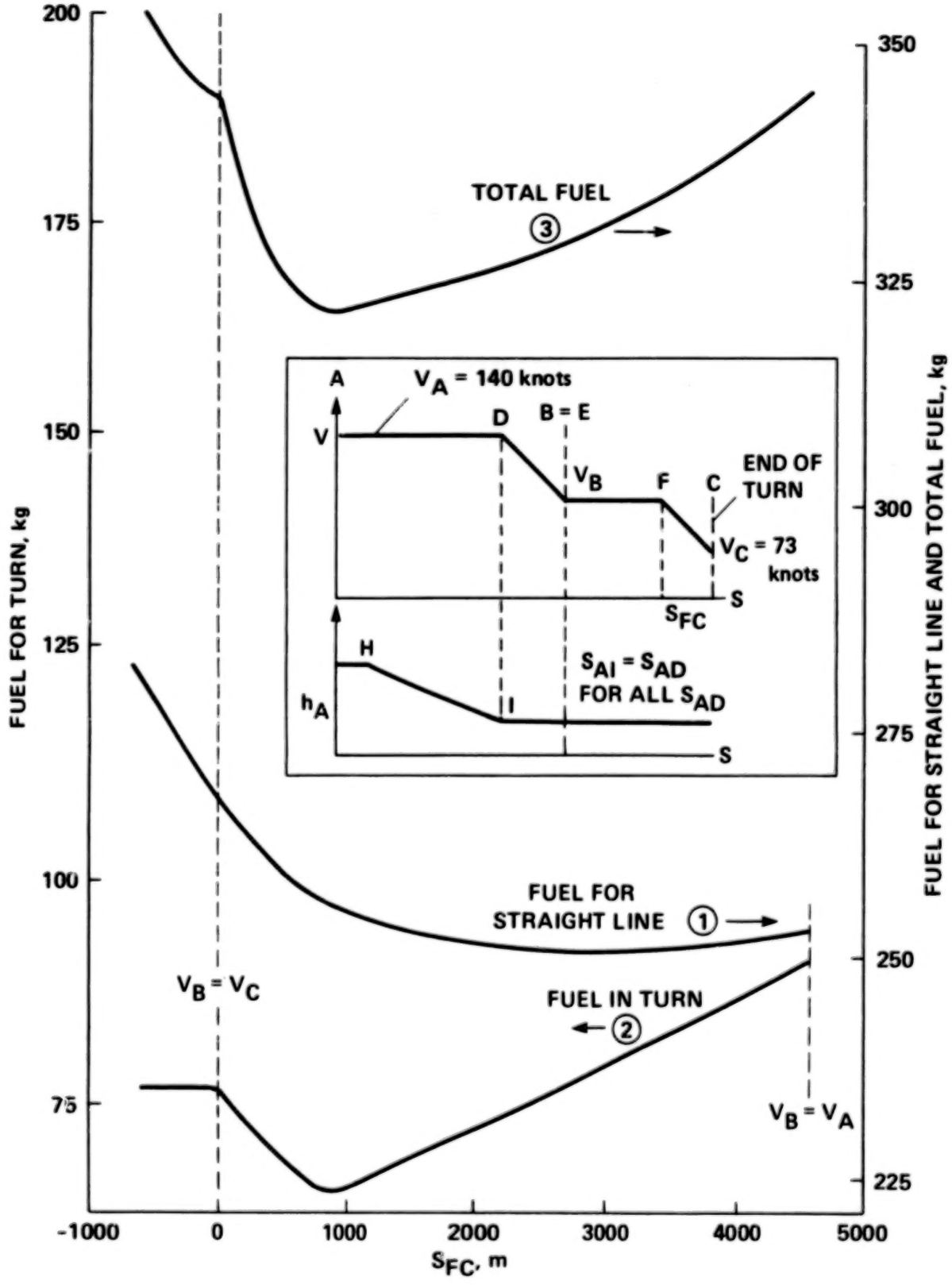

Figure 12.- Fuel for a two-deceleration approach vs S_{FC} (no wind), $\gamma_I = 7°$, a = -0.042 g, $S_{AI} = S_{AD}$.

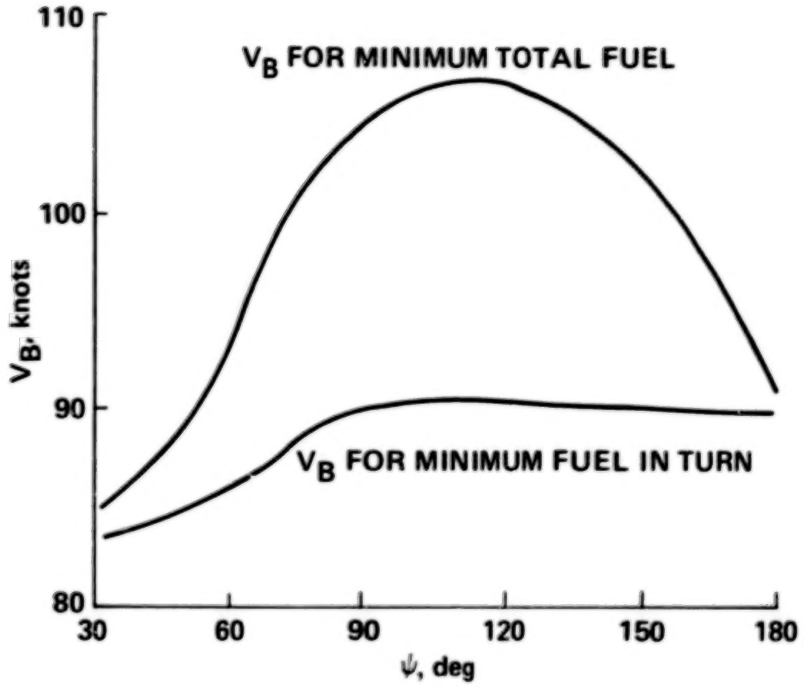

Figure 13.- V_B vs ψ (no wind), V_A = 140 knots, V_C = 73 knots.

Results for All Approaches

We have now developed a feeling of how fuel consumed varies in individual segments and in particular examples of approaches, and we shall give the results for the data matrix discussed earlier. The data for the approaches with six different approach angles are tabulated in table 1. All distances shown are measured from Point B, the beginning of the turn. Columns 1 to 10 describe the minimum fuel approaches where the descent is finished at the end of the turn. Columns 11 to 12 describe the changes that occur when the point of descent is allowed to move to minimize fuel. The resulting minimum fuel approach would have larger community noise effects, however.

The parameter that best describes the optimal flightpath by a single number is the velocity at the start of the turn V_B. The other parameters in table 1 can be directly calculated from V_B, the boundary values (V_A, V_C, etc.), and the winds. Hence, V_B is plotted in figure 14 for various terminal conditions and zero wind, and the shaded area indicates the change of V_B for different winds and flightpaths for the nominal conditions (heavy line). The shaded area shows a maximum at about $\psi = 60°$; it becomes narrower for large-turn angles, where the tailwinds in the turn vary in magnitude and sign in a compensating manner. For turns less than 90°, the optimal speed profile is a single deceleration segment ($S_{BF} = 0$), which begins before the turn and terminates at the end of the turn. For other terminal conditions, even at zero wind, V_B shows large variations, so that on-board implementation of V_B calculations via table lookup would be difficult. Columns 5, 6, and 10 show that both the start of the deceleration segments and the fuel used are sensitive functions of the winds. The total fuel varies mostly as function of the

TABLE 1.- ANALYTICAL RESULTS FOR MINIMUM FUEL APPROACHES,
X = 21,336 m, a = -0.042 g, V_A = 140 knots, V_C = 75 knots

Winds		Turn angle	Minimum fuel approaches, finish descent at end of turn							Descent for minimum fuel	
W_x, knots (1)	W_y, knots (2)	γ, deg (3)	R, m (4)	S_{DB}, m (5)	S_{BF}, m (6)	S_{BC}, m (7)	V_B, knots (8)	t, sec (9)	f, kg (10)	f, kg (11)	S_{IB}, m (12)
0	0	30	787.8	4082.7	0.0	412.5	83.1	315.3	269.7	266.7	4082.7
-40			926.3	2519.5		485.0	91.8	421.7	363.6	361.9	2519.5
-25			850.6	3125.9		445.4	87.1	374.4	321.5	319.4	3125.9
0			773.0	4456.8		404.8	82.1	296.6	253.4	250.2	4456.8
0	-15		794.6	3786.8		416.0	83.6	333.2	285.3	282.6	3786.8
0	15		781.9	4379.7		409.4	82.7	299.3	255.6	252.4	4379.7
0	0	60	953.4	3496.8	0.0	998.4	93.4	317.5	272.0	269.2	3496.8
-40			1264.3	1990.5		1324.0	110.6	378.6	324.7	323.1	1990.5
-25			1098.7	2665.8		1150.6	101.8	352.4	301.8	299.9	2665.8
0			918.2	3778.9		961.6	91.3	305.6	262.0	258.8	3778.9
0	-15		988.4	2999.3		1035.1	95.5	350.1	300.6	298.2	2999.3
0	-15		925.8	3998.5		969.5	91.8	290.3	248.3	245.1	3998.5
0	0	90	1172.2	2706.0	52.1	1841.2	105.8	324.6	278.5	275.7	2706.0
-40			1264.3	2368.5	662.0	1986.0	110.6	339.2	288.6	288.2	2368.5
-25			1256.3	2397.9	328.9	1973.4	110.2	332.3	283.3	282.1	2397.9
0			1136.6	2835.6	.0	1785.4	103.8	322.5	277.4	274.1	2835.6
0	-15		1236.9	2171.7	105.6	1943.0	109.2	364.5	313.6	311.3	2171.7
0	15		1122.7	3442.2	.0	1763.6	103.1	292.4	250.4	242.4	3242.2
0	0	120	1186.1	2655.0	644.0	2484.2	106.5	338.1	290.6	288.5	2655.0
-40			1188.3	3076.2	1370.2	2488.8	106.6	314.0	266.0	265.5	2258.3
-25			1188.3	2915.2	1061.0	2488.9	106.6	320.5	272.8	272.0	1867.6
0			1188.3	2539.6	509.5	2488.8	106.6	347.3	299.8	296.9	2539.6
0	-15		1189.2	2363.8	808.6	2491.7	106.7	374.5	332.7	321.7	-1629.7
0	15		1188.3	2925.7	458.8	2488.9	106.6	308.1	264.4	261.9	2925.7
0	0	150	1081.2	3036.7	1372.2	2830.6	100.8	354.3	306.4	304.1	-1591.6
-40			1146.1	3595.2	1992.2	3000.5	104.4	306.3	260.1	259.3	-2486.9
-25			1098.7	3505.7	1725.9	2876.5	101.8	319.2	273.5	272.0	-2048.8
0			1086.2	2801.8	1247.9	2843.6	101.1	373.2	324.2	321.1	-1363.0
0	-15		1095.9	2798.3	1489.6	2869.1	101.6	378.4	327.2	325.0	-1763.0
0	15		1107.6	3123.3	1197.6	2899.6	102.3	333.7	288.7	286.0	-1453.5
0	0	180	944.4	3529.0	2000.7	2966.9	92.9	370.4	323.2	320.7	3529.0
-40			948.7	4210.2	2529.3	3294.7	99.0	312.6	268.5	268.0	2582.2
-25			958.2	4223.8	2271.7	3610.4	93.7	327.3	283.6	282.5	4223.8
0			970.9	3141.3	1888.9	3050.1	94.5	394.4	345.6	341.9	3141.3
0	-15		928.0	3587.6	2072.9	2915.3	91.9	377.6	328.9	327.1	3587.6
0	15		961.0	3469.7	1908.9	3019.0	93.9	364.8	319.3	316.0	3469.1

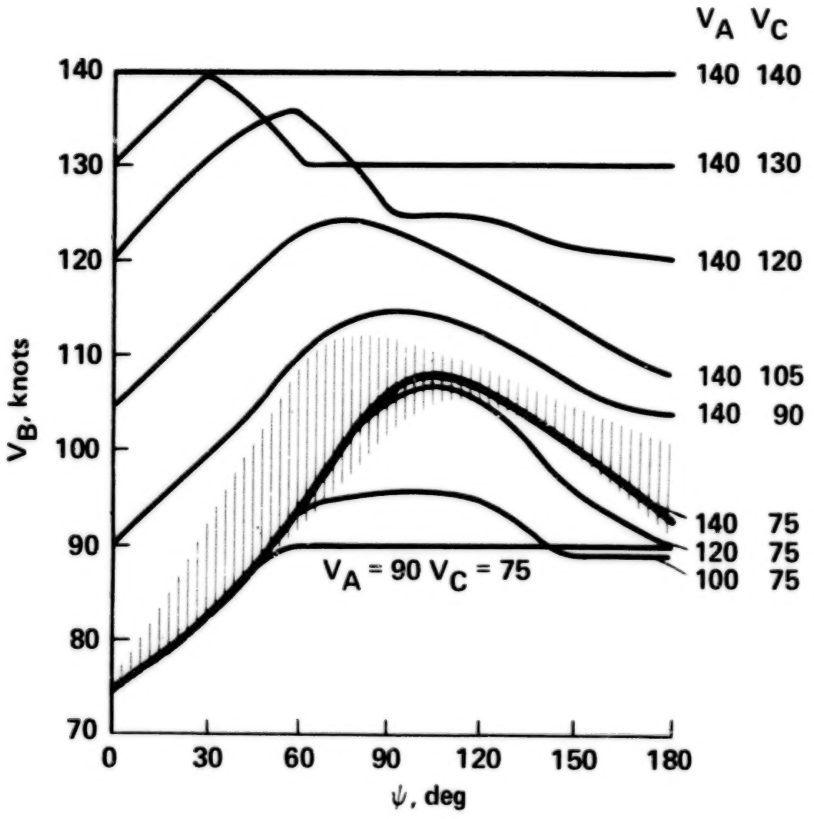

Figure 14.- Range of V_B for different ψ and different terminal conditions.

tailwind in the straight-line segment. For instance, for $\psi = 180°$, the fuel used varies from 269 kg for a 40-knot tailwind to 345 kg for a 10-knot headwind. Note that the results in columns 5 and 12 are equal for many of the cases studied. This indicates that for minimum fuel consumption the descent should end before the beginning of the first deceleration. But, as can be seen by comparing columns 10 and 11 of table 1, descending as late as possible, thus reducing community noise, costs no more than 3 kg of fuel.

We will now compare the two deceleration minimum fuel approaches with other types of approaches, using the data shown in table 2. First, the two-deceleration-segment approach will be compared to the minimum-radius turn approach. The latter has a single deceleration segment that terminates just at the beginning of the turn. Column 3 of table 2 and curve 1 of figure 15 show that for turns $\psi > 90°$ this approach uses up to 29 kg (or 21 kg for zero wind) more fuel than the fuel-optimum two-deceleration-segment approach. As shown in column 4, the minimum-radius turn approach usually takes more time than the minimum-fuel approach. Second, the minimum-time, two-deceleration-segment approach (table 2, columns 5-9) will be compared with the minimum-fuel approach. Since no initial acceleration was allowed, the minimum time approach usually saved less than 2 sec (column 9) and costs very little extra in terms of fuel (column 8) when compared to the fuel-optimum approach. An appreciable difference in the fuel used occurs only in the 180° turn. This

TABLE 2.- COMPARISON OF OTHER TYPES OF APPROACHES WITH RESULTS FOR MINIMUM FUEL, X = 21,336 m, a = -0.042 g, V_A = 140 knots, V_C = 75 knots

Winds		Turn angle	Minimum radius turn approach[a]				Minimum time approach[a]				
W_x, knots	W_y, knots	γ, deg	f, kg (1)	t, sec (2)	Δf, kg (3)	Δt, sec (4)	S_{BF}, m (5)	f, kg (6)	t, sec (7)	Δf, kg (8)	Δt, sec (9)
0	0	30	277.4	319.5	7.7	4.2	0.0	269.7	315.3	0.0	0.0
40			380.3	432.4	16.7	10.7		363.6	421.7		
-25			332.2	381.4	11.7	7.0		321.5	374.4		
10			260.2	300.1	6.8	3.5		253.4	296.6		
0	-15		293.5	337.8	8.2	4.6		285.3	333.2		
0	15		262.9	303.1	7.3	3.8		255.6	299.3		
0	0	60	287.0	325.2	15.0	7.7	0.0	272.0	317.5	0.0	0.0
-40			350.7	392.5	26.0	13.9		324.7	378.6		
-25			322.0	363.0	20.2	10.6		301.8	352.4		
10			275.6	312.5	13.6	6.9		262.0	305.6		
0	-15		317.4	359.4	16.8	9.3		300.6	350.1		
0	15		262.0	296.9	13.7	6.6		248.3	290.3		
0	0	90	298.6	333.0	20.1	8.4	0.0	278.9	324.6	0.0	0.0
-40			317.6	349.3	29.0	11.1	708.7	288.7	339.0	.1	-.2
-25			307.5	340.8	24.2	8.5	406.9	283.5	332.2	.2	-.1
10			296.4	330.9	19.0	8.5	.0	277.4	322.5	.0	.0
0	-15		336.4	374.9	22.8	10.4	72.8	313.7	364.5	.1	.0
0	15		268.7	299.5	18.3	7.1	.0	250.4	292.4	.0	.0
0	0	120	312.3	343.3	21.7	5.2	812.5	291.1	337.9	0.5	-0.2
-40			295.4	319.1	29.4	5.1	1437.9	267.4	313.3	1.4	-.7
-25			297.7	324.6	24.9	4.1	1217.4	274.0	319.9	1.2	-1.0
10			320.8	353.2	21.8	5.9	650.3	300.0	347.2	.2	-.1
0	-15		347.8	381.8	25.1	7.3	887.5	323.0	374.4	.3	-.1
0	15		284.0	312.1	19.6	4.0	727.8	265.1	307.7	.7	-.4
0	0	150	327.8	355.8	21.4	1.5	1542.6	307.5	353.4	1.1	-0.9
-25	0		296.6	319.0	23.5	-.2	1781.4	277.0	317.3	3.9	-1.9
10	0		345.5	375.1	21.3	1.9	1411.6	324.9	372.6	.5	-.6
0	-15		352.3	381.3	25.1	2.9	1570.2	328.1	377.7	.9	-.7
0	15		307.7	334.2	19.0	.5	1511.1	290.3	332.4	.5	-1.3
0	0	180	343.9	369.5	20.7	-0.9	2070.0	332.5	369.0	9.3	-1.4
-25	0		305.4	325.0	21.8	-2.3	2152.0	297.0	324.7	13.4	-2.6
10	0		366.4	394.2	21.4	-.2	2002.3	250.9	393.3	5.9	-1.1
0	-15		353.8	377.7	24.9	.1	2080.2	226.5	376.8	7.6	-.8
0	15		337.6	363.5	18.0	-1.3	2063.6	326.3	363.2	7.0	-1.6

[a] Δ denotes comparison with minimum fuel approach, for example, $\Delta f = f_{\text{min time}} - f_{\text{min fuel}}$.

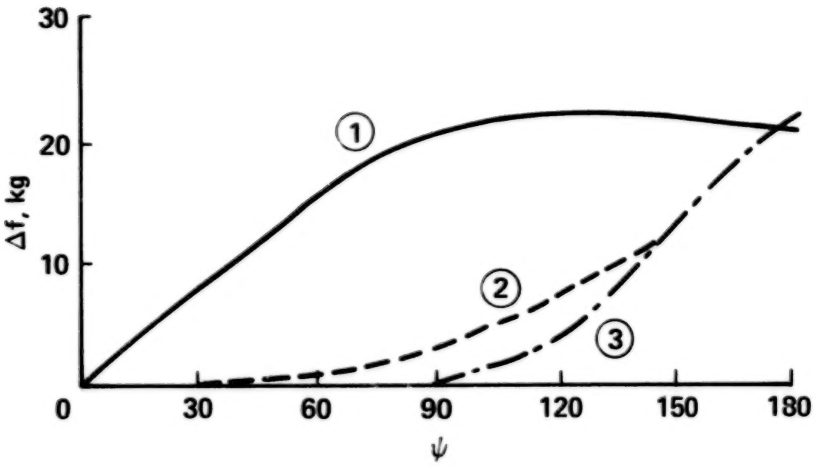

① EXCESS FUEL USED WHEN DECELERATION COMPLETED AT BEGINNING OF TURN $R=R_{min}$

② EXCESS FUEL USED WHEN DECELERATION COMPLETED AT END OF TURN $R=R_{max}$

③ EXCESS FUEL USED WHEN DECELERATION COMPLETED AT END OF TURN $R=f(V_B)$

Figure 15.- Fuel cost for single-deceleration strategies, compared to optimal two-deceleration strategy (no wind).

means that one could implement the much simpler minimum-time calculations and would still obtain (or nearly so) the benefit of minimum fuel.

It was found that fuel consumption was insensitive to the descent angle used. The flights shown in table 1 were repeated for $\gamma_I = -3°$ and for $\gamma_I = -1°$. As compared to the results for $\gamma_I = -7°$ at $-3°$, 3 kg of fuel is saved when descending at the end of the turn and only 1 kg of fuel when choosing the descent for minimum fuel. Another 0.5 kg gain occurs when going to $\gamma_I = -1°$. Such small gains are insignificant, especially when considering that the mathematical model of the aircraft did not include the effect of altitude on fuel consumption (which would favor flight at a higher altitude, thus reversing the above trend).

The fuel consumption was only moderately sensitive to the magnitude of deceleration. Data are given in table 1 for a deceleration of 0.042 g. When repeating the 36 flights with decelerations of 0.031 g and 0.050 g, the fuel consumption increases on the average by 5.5 kg or decreases by 3.2 kg, respectively. This agrees with an earlier observation that, with all else equal, the higher the deceleration, the less fuel is used. Since winds are not exactly known, however, a margin of deceleration capability must be preserved. As shown above, this margin incurs a small cost in fuel.

If results of this work are used off-line in the specification of fixed approach paths, extra fuel will be needed to design wind-proofed flightpaths. To determine how much extra fuel is needed, for simplicity, the straight flightpath will be examined, as illustrated in figure 16. The difference in

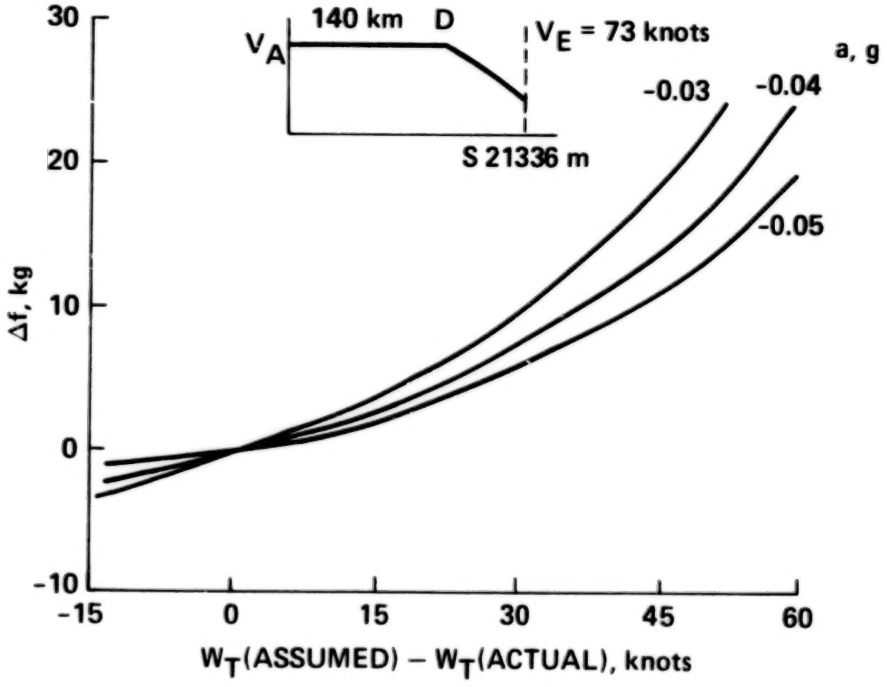

Figure 16.- Fuel penalty vs wind estimation errors for different nominal decelerations for a conservative flightpath design.

fuel was calculated when Point D was calculated from equation (2) for the actual tailwind and for the assumed tailwind of 30 knots for a wind-proofed design. The fuel penalty for flying the wind-proofed path is shown in figure 16. It is plotted for $\gamma_I = 0$ only, since f is nearly independent of γ_I. There is a fuel saving if the actual tailwind is larger than the design tailwind (however, such errors strain the deceleration capability of the aircraft) and a rapidly rising extra fuel expenditure when the actual tailwind is more than 15 knots less than the design tailwind. This is due to the aircraft decelerating at a lesser rate than necessary. If the results of this work are used for on-board optimization, then the abscissa in figure 16 is the wind estimation error. Hence, on-board optimization is desirable.

Another comparison is with the fuel conservative system of Erzberger and McLean (ref. 4). Briefly, the system incorporates two types of flightpaths in sequence. First, it has a turn-straight-turn, so-called capture flightpath, which connects any aircraft position, speed, altitude, and heading to any specified (capture) way point on a fixed flightpath. Second, it has fixed flightpaths, which are specified by way points. Way points are defined by position, heading, speed, and turn radius of the following segment. For the

capture flightpath, the system minimizes fuel while meeting the capture way point conditions. For the fixed flightpath, the system minimizes fuel between adjacent way points, while attempting to meet the specified conditions at the way points.

The Erzberger-McLean system uses optimization results obtained for straight flightpaths as approximations for the actual curved flightpaths. Hence the system's capture flightpath has a single deceleration at the end of the final turn with a radius appropriate to the 140-knot approach speed. Curve 2 of figure 15 compares this with the two-deceleration segment profile, provided that the initial aircraft heading is such that the general turn-straight-turn capture trajectory results in a single turn at the end of the flightpath. Curve 2 shows that the procedure does not deviate much from the optimum for turns less than 90°. The difference between curves 2 and 3 shows the relatively small improvement that can be obtained by the change of varying R according to equation (4) in the single-deceleration system of Erzberger and McLean. The full implementation of the two-deceleration segments in the flight system of reference 4 would significantly increase the computation time, since the optimal airspeed and horizontal profiles must be determined iteratively. However, the insight gained in this investigation can be directly applied to the fixed flightpath portion of the system. One simply specifies a reference flightpath with proper R and V_B from the results in this report, and the speed profile selected between A and C of figure 2 will be optimized by separately optimizing A-B and B-C. This idea carries to more complex terminal area approaches, which are usually constructed of a succession of long straight segments followed by constant radius turns.

Flight-Test Verification of Analytical Results

As a check, for $\psi = 180°$, three types of approaches were flown: the minimum airspeed approach, the fuel optimum two-deceleration segment approach, and the single deceleration approach that terminates deceleration at the end of the turn. These tests were flown in the Augmentor Wing Aircraft on a calm day (August 7, 1979) at Crows Landing Naval Air Station. The aircraft was equipped with STOLAND (ref. 7), which used the airborne computer program of reference 4. On the average, the minimum-fuel turn used 27 kg less of fuel than the approach in which deceleration occurs last, and 23 kg less than the minimum-airspace approach. This result agrees well with the values predicted in this report.

Analytical Results for a CTOL Jet

There is presently great interest in fuel-efficient operation of CTOL aircraft (ref. 8). Therefore, the method described in this report was also applied to the final approach of the Boeing 727. The energy-rate diagram for the aircraft at a weight of 56,700 kg, an altitude of 914.4 m, and bank angles of 0° and 20° is given in figure 17. To have an adequate maneuver margin, the fuel flow values at each point on the diagram are given for the

minimum throttle and minimum flap settings that will result in an angle of attack of less than or equal to 8°. It will be noticed that, compared to the Augmentor Wing, the Boeing 727 has less drag and, consequently, a much smaller negative $\dot{E}_n$ capability. It is therefore not possible to descend at -3° and decelerate at 0.05 g simultaneously. From results discussed in this paper, it is meaningful to investigate instead a constant speed -3° descent from

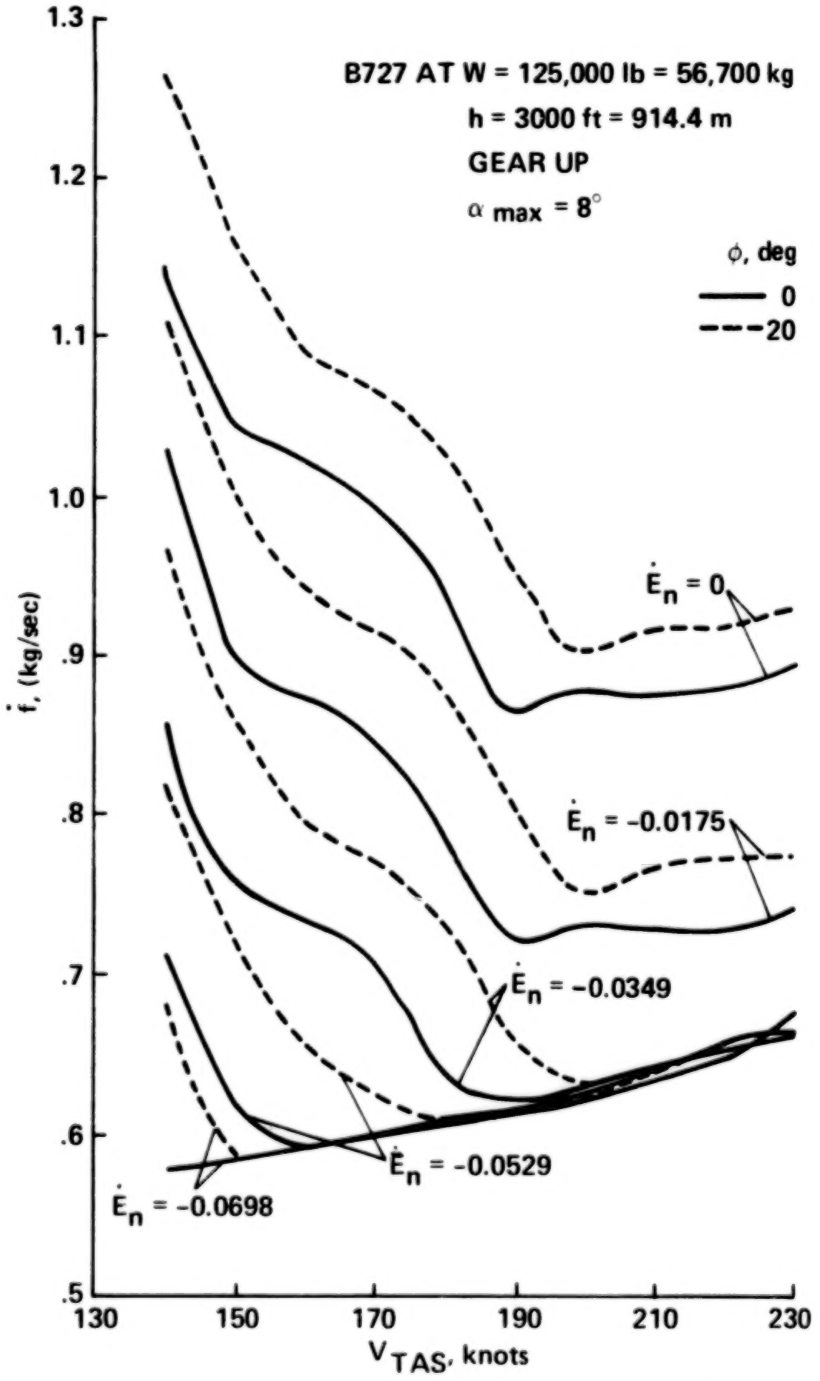

Figure 17.- Fuel flow rate vs airspeed for the Boeing 727 at an altitude of h = 914.4 m, and at an aircraft weight of 56,700 kg.

914.4 m to 279.5 m that is immediately followed by level flight and deceleration from 230 knots terminal area speed to 140 knots landing airspeed. Abbreviated results for the no-wind case are given in figure 18. The general shapes of the curves are similar to those given for the Augmentor Wing. Indeed, the fuel savings for the two-deceleration strategy for the Boeing 727

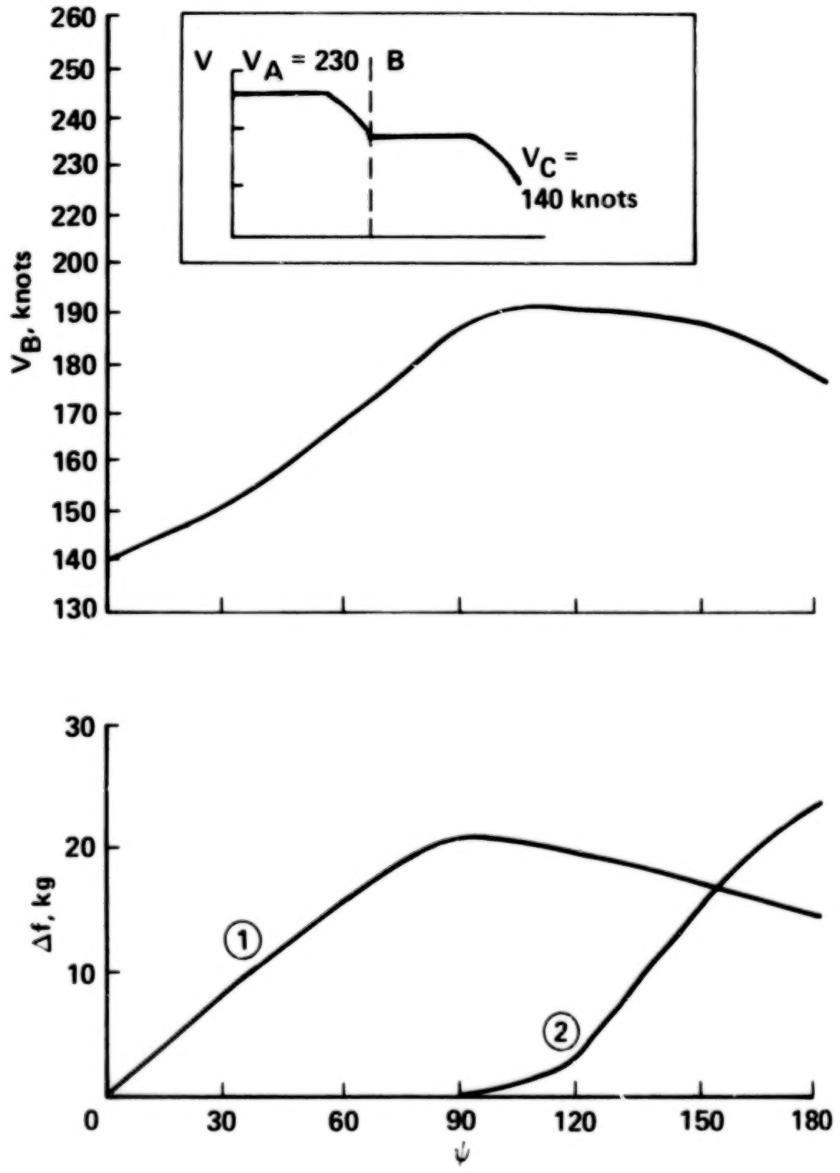

Figure 18.- The two-deceleration strategy for the Boeing 727 and a comparison to single-deceleration strategies.

are almost the same as for the Augmentor Wing Aircraft. For the range of winds considered for the Augmentor Wing, the trends of the data are similar and will not be presented here.

SUMMARY AND CONCLUSIONS

This paper has described a method for determining fuel-conservative terminal approaches that include changes in speed, heading, and altitude. The horizontal approach trajectory is constrained to a straight segment followed by a constant-radius turn; the vertical trajectory is constrained to level flight plus one segment with constant inertial flightpath angle; and the speed profile is constrained to a maximum of two deceleration segments. Results for the Augmentor Wing Jet STOL Research Aircraft and for the Boeing 727 indicate that for either minimum fuel or minimum time, two deceleration segments are required, one terminating at the end of the straight-line approach and the other at the end of the turn. For small heading changes, these collapse to a single deceleration segment ending at the end of the turn. Minimum-time and minimum-fuel trajectories do not differ much, since accelerations were not permitted, and at the initial high speed, the fuel consumed per unit distance was minimum. In contrast, for minimum airspace (minimum turn radius), a single deceleration segment is required just before the turn. Airspace is minimized at a fuel cost of about 21 kg more than the optimal two deceleration segment approach. For minimum fuel consumption, deceleration should always be at the highest practical rate. The choice of a specific glide-slope angle has a small effect on the total amount of fuel consumed. To minimize fuel consumption, for most conditions, the descent should be completed before initiating the first deceleration. However, choosing the descent to terminate at the end of the turn, in order to minimize community noise, results in a fuel penalty of only a few kilograms. Two deceleration segment profiles can be easily calculated off-line for existing research RNAV systems, such as those described in references 1 and 4, with some saving of fuel. On-board implementation to consider measured winds will be more difficult.

Ames Research Center
National Aeronautics and Space Administration
Moffett Field, Calif., 94035, October 2, 1979

APPENDIX

ADDITIONAL FUEL SAVINGS THROUGH VARIABLE RADIUS TURNS

In the approaches discussed in the body of the report, the final turn of the aircraft (which aligns the aircraft and runway heading) is made as a constant radius turn even while the aircraft decelerates. A properly chosen constant bank angle turn approach or an approximation of such an approach can save additional fuel when compared to the minimum fuel constant radius turn approach. The exact constant bank angle approach for $\psi = 180°$, shown in figure 19(a), consists of a curve defined by its instantaneous radius

$$R = V^2/(g \tan \phi) \text{ (m)} \tag{A1}$$

where ϕ is chosen smaller than the nominal 20° to provide a bank angle margin sufficient to handle W = 20-knot tailwind

$$\tan \phi = V_{min}/(V_{min} + W))^2 \tan 20° \tag{A2}$$

(Note: defining $R = (V + W)^2/(g \tan \phi)$ for constant wind-proofing did not result in a closed form solution.) The approximation of the constant bank angle turn, shown in figure 19(b), consists of a sequence of constant radius turn segments, where the radius R_j of each turn segment is determined by the entry speed V_j to the jth segment and the desired windproofing

$$R_j = (V_j + W)^2/(g \tan 20°) \text{ (m)} \tag{A3}$$

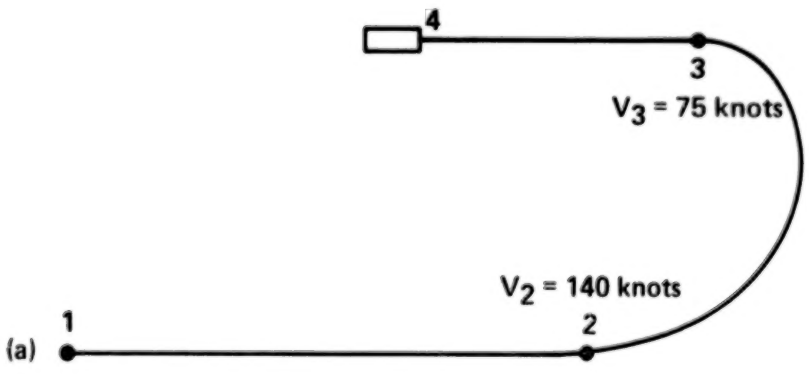

(a) Constant bank angle turn approach for zero wind.

Figure 19.- Minimum fuel constant bank angle turns.

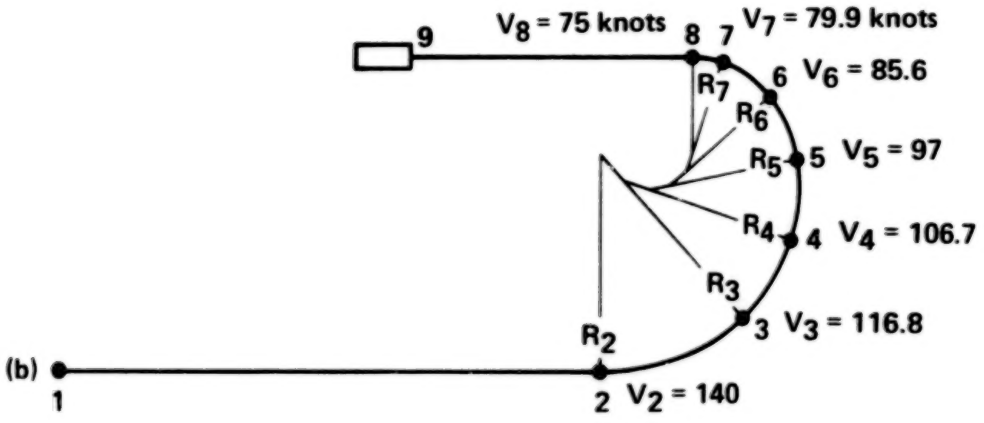

R_2 = 1604 m, R_3 = 1381 m, R_4 = 1168 m,

R_5 = 1017 m, R_6 = 846 m, R_7 = 739 m

(b) Approximation of constant bank angle turn approach.

Figure 19.- Concluded.

For the 180° turn, a set of six such segments gives an adequate approximation of the exact constant bank angle trajectory. The curved portion of the approach begins with a constant radius turn for the constant speed portion, followed by a constant or approximately constant bank angle turn for the decelerating portion. The additional fuel savings are shown in figure 20, for the type of approach shown in figure 19(b). The savings are similar for the type of approach shown in figure 19(a). The resulting minimum fuel turns have essentially a single deceleration speed profile with the deceleration ending at the end of the turn. This indicates that if the turn is executed

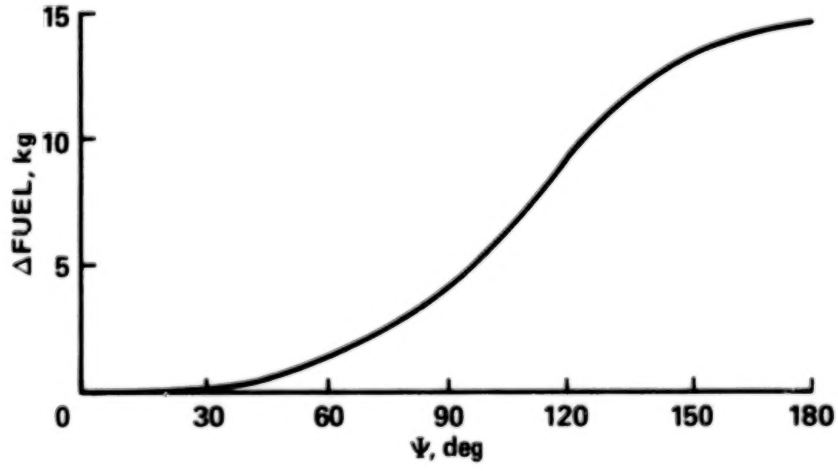

Figure 20.- Fuel saving of minimum fuel constant bank angle turn approach compared to minimum fuel constant radius turn approach.

in an optimal fashion, the original result for the straight approach applies — decelerate as late as possible. However, to save this amount of fuel, one requires additional way points (fig. 19(b)) or additional programming complexity (fig. (19(a)) to define the equation for the constant bank angle turn. Airspace usage, if measured by the distance between the two straight segments, has also increased compared to the fuel minimum two-deceleration constant radius approach, 2343 m vs 1888 m.

The 180° approach of figure 19(b) was flown three times. For fuel comparison, an equivalent capture trajectory (ref. 4) was also flown twice from way point 1 to the capture way point 8. The average amount of fuel saved for the constant bank angle turn was 31 kg. This is in reasonable agreement with the sum of the fuel savings as shown in curve II of figure 16 and in figure 20.

REFERENCES

1. Neuman, Frank; Warner, David N.; and Moran, Francis J.: A Flight Investigation of a 4D Area Navigation System Concept for STOL Aircraft in the Terminal Area. NASA TM X-73,195, 1977.

2. Neuman, Frank; and Lee, Homer Q.: Flight Experience with Aircraft Time of Arrival Control. Journal of Aircraft, vol. 14, no. 2, Feb. 1977.

3. Lee, Homer Q.; and Neuman, Frank: 4D Area Navigation System Description and Flight Test Results. NASA TN D-7874, 1975.

4. Erzberger, Heinz; and McLean, John D.: Fuel Conservative Guidance System for Powered Lift Aircraft. AIAA Guidance and Control Conference, Boulder, Colorado, Aug. 1979.

5. Bryson, Arthur E., Jr.; and Ho, Yu-Chi: Applied Optimal Control. Blaisdell Publishing Company, 1969.

6. Jacob, Heinrich G.: An Engineering Optimization Method with Application to STOL Aircraft Approach and Landing Trajectories. NASA TN D-6978, 1972.

7. Neuman, Frank; Watson, DeLamar M.; and Bradbury, Peter: Operational Description of an Experimental Digital Avionics System for STOL Airplanes. NASA TM X-62,448, 1975.

8. Erzberger, Heinz; McLean, John D.; and Barman, John F.: Fixed Range Optimum Trajectories for Short-Haul Aircraft. NASA TN D-8115, 1975.

1. Report No.	2. Government Accession No.	3. Recipient's Catalog No.
NASA TP-1650		

4. Title and Subtitle	5. Report Date
ANALYSIS OF FUEL-CONSERVATIVE CURVED DECELERATING APPROACH TRAJECTORIES FOR POWERED-LIFT AND CTOL JET AIRCRAFT	April 1980
	6. Performing Organization Code
7. Author(s)	8. Performing Organization Report No.
Frank Neuman	A-7986
	10. Work Unit No.
9. Performing Organization Name and Address	532-02-11
Ames Research Center, NASA Moffett Field, Calif. 94035	11. Contract or Grant No.
	13. Type of Report and Period Covered
12. Sponsoring Agency Name and Address	Technical Paper
National Aeronautics and Space Administration Washington, D.C. 20546	14. Sponsoring Agency Code

15. Supplementary Notes

16. Abstract

This paper describes a method for determining fuel-conservative terminal approaches that include changes in altitude, speed, and heading. The horizontal approach trajectory is constrained to a straight segment followed by a constant radius turn; the vertical trajectory is constrained to level flight plus one descending segment with constant inertial flightpath angle; and the speed profile is constrained to a maximum of two deceleration segments. Simulation results for the Augmentor Wing Jet STOL Research Aircraft and for the Boeing 727 aircraft indicate that for minimum fuel consumption, two deceleration segments are required: one terminates at the end of the straight-line approach and the other at the end of the turn. Deceleration should be at the highest practical rate for minimum fuel consumption. The choice of a specific glide-slope angle has a small effect on the total amount of fuel consumed as long as the altitude change is small. For most conditions, the descent should be completed before the first deceleration is started. However, choosing the descent to terminate at the end of the turn in order to minimize community noise levels results in a penalty of only a few kilograms of fuel. For comparison, a trajectory optimized for a single deceleration segment requires about 21 kg more fuel than the optimal two-deceleration approach. These results were verified by flight tests using the Augmentor Wing Aircraft. Additional fuel savings possible through variable radius turns are discussed in the appendix.

17. Key Words (Suggested by Author(s))	18. Distribution Statement
Fuel conservative approaches 3-D RNAV Minimum fuel speed profiles	Unclassified - Unlimited STAR CATEGORY - 01

19. Security Classif. (of this report)	20. Security Classif. (of this page)	21. No. of Pages	22. Price*
Unclassified	Unclassified	39	$4.50

*For sale by the National Technical Information Service, Springfield, Virginia 22161

NASA-Langley, 1980

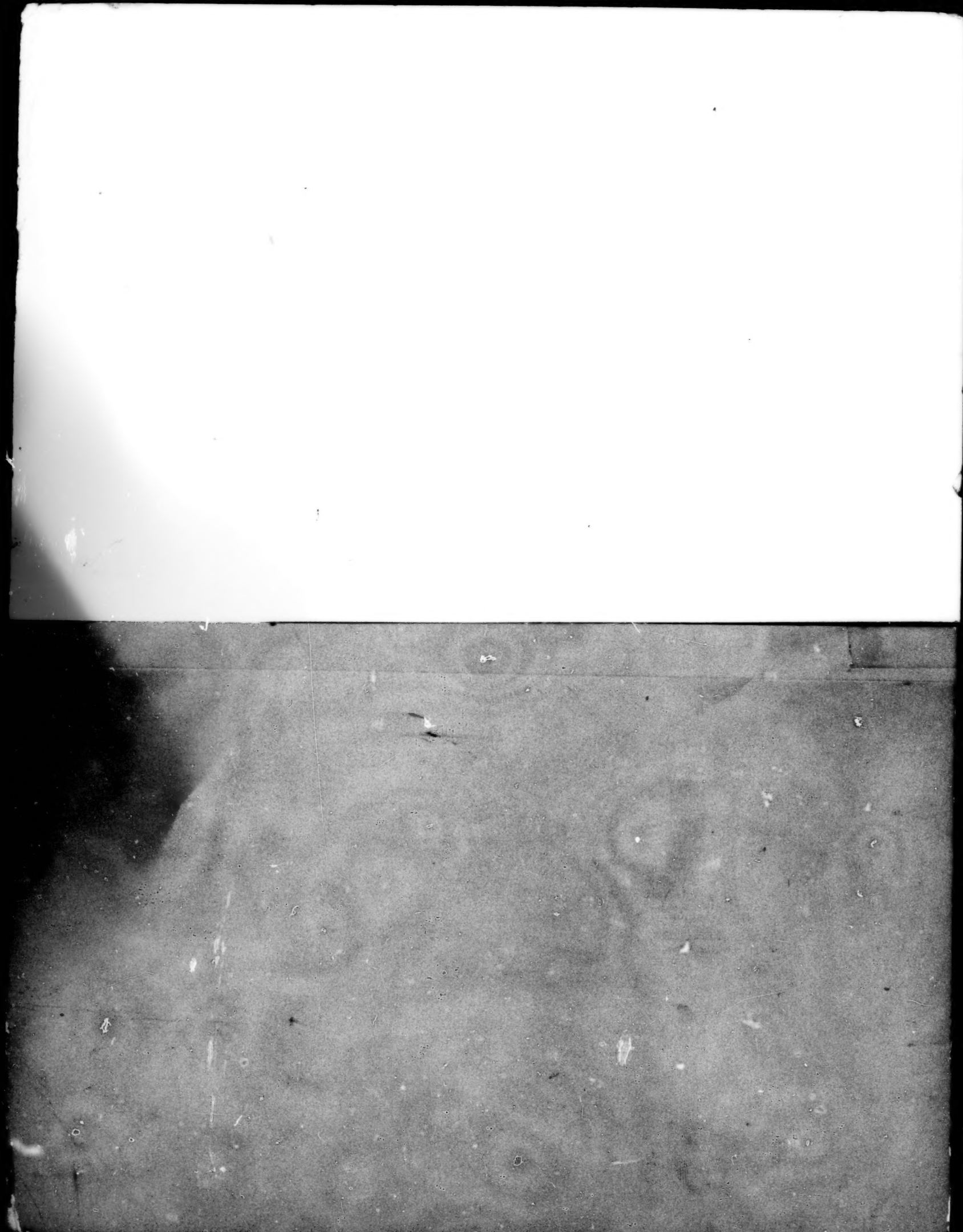

END

June, 29, 1981